16th World Conference on Earthquake, 16WCEE 2017
Santiago Chile, January 9th to 13th 2017
Paper N° 1649 (Abstract ID)
Registration Code: S-N1463288913

ANALYSIS OF TANK ROCKING MOTION BASED ON A SPRING-MASS-RIGID-BODY COMBINED MODEL AND MAGNIFICATION FACTOR

T. Taniguchi[(1)], D. Okui[(2)], T. Nakashima[(3)], Y. Yoshida[(4)]

[(1)] *Professor, Tottori University, t_tomoyo@cv.tottori-u.ac.jp*
[(2)] *Engineer, Kawasaki Heavy Industries, Ltd., okui_daisuke@khi.co.jp*
[(3)] *Manager, JIP Techno-Science, teruhiro_nakasima@cm.jip-ts.co.jp*
[(4)] *Graduate student, Tottori University, M14T6018B@edu.tottori-u.ac.jp*

Abstract

For the unanchored flat-bottom cylindrical tanks located in the seismically active area, uplift of the tank bottom plate is inevitable. This paper proposes the use of a mechanical model consisting of a spring-mass-rigid body combined system for analyzing the seismic response of the unanchored flat-bottom cylindrical tank that is set on the almost rigid foundation, pivots on either bottom edge and has a crescent-like uplift region of the tank bottom plate. Since its equation of motion naturally incudes interaction between the fluid moving in unison with the tank rocking motion and that moving in unison with the tank bulging motion, this paper employs the effective mass of fluid for rocking motion, that for bulging motion and that for rocking-bulging interaction derived by solving a boundary-value problem with the boundary conditions corresponding to the tank rocking motion and the tank bulging motion, respectively. The equation of motion is rearranged to include the corresponding effective masses of fluid and a response magnification factor. By ordering some terms of it, the simplified calculation that enables to approximate the maximum angular acceleration of the tank rocking motion, the absolute maximum response acceleration of the tank bulging motion, the maximum base shear and the maximum reactions at a pivoting bottom edge is derived. Consider a tank with the undeformable cylindrical shell subjected to the harmonic base excitation whose driving period is the same as the natural period of the tank bulging motion, the analytical accuracy of the proposed method is examined. Although out-of-round deformation of the tank shell enlarges the uplift displacement of tanks, its consideration remains as future work. Comparison between results of the proposed method and that of the explicit finite element analysis reveals that the proposed method may approximate the angular acceleration accompanying the tank rocking motion, if de-amplification of the tank rocking motion due to landing of the tank bottom plate on the foundation is properly taken into account.

Keywords: uplift; effective mass of fluid; rocking-bulging interaction; response spectra; angular acceleration

1. Introduction

For cylindrical tanks, which are not anchored to the foundation, in the seismically active area, uplift of the tank bottom plate is inevitable due to the seismic overturning moment. Analyzing the tank rocking motion has been subject of many researchers [for instance, 1 and 2]. However, since its dynamical mechanism was not clearly clarified to date, the tank rocking motion has not been enjoyed any analytical treatments. Employing numerical analyses or shaking table experiments, its qualitative evaluation has been made. Even seismic design code, uplift of the tank bottom plate is determined by a diagram derived from a parametric study with finite element model tanks as a function of the overturning moment for different values of the aspect of the tank [3]. Complexity of the tank rocking motion, which discontinuously appears during earthquake, may be reluctant to apply analytical treatment to it. However, to produce cylindrical tanks with appropriate safety margin at the severe earthquake events, development of the concise but easy method of analyzing the tank rocking motion is indispensable.

On the analogy of the rocking motion of the two degree of freedom (2DOF) model consisting of a spring-mass system and another mass attached to its bottom, Taniguchi [4] presented a mechanical model that may describe the tank rocking motion. Following the manner of Ref. [5], the first part of this paper derives the equations of motion for the 2DOF model through variational approach. The essence of the equation of motion is that the rotational inertia force and the centrifugal force acting on a vibrant mass of the spring-mass system accompanying the rocking motion of the 2DOF model is naturally included. In addition, an interaction between translational and rocking motions of the 2DOF model explicitly appears. The second part of the paper derives the equation of motion of the tank rocking motion by replacing the masses, spring constant and moment inertias of the 2DOF model in the equation of motion for corresponding physical quantities governing the tank bulging motion, i.e. response of a combined tank-liquid system, and the rocking motion. This study employs the effective mass for rocking motion, its moment inertia and the effective mass for rocking-bulging interaction defined by solving a boundary value problem of fluid moving in unison with the tank rocking and/or bulging motions [6]. The third part of the paper simplifies the equation of motion of the tank rocking motion by assuming that a value of response acceleration spectra may give the response of the tank bulging motion in the absence of uplift and by ignoring some forces according to their effects on the response of interest. To examine analytical accuracy of the proposed method, the last part of the paper compares the angular acceleration accompanying the tank rocking motion calculated by the proposed method and that computed by the explicit finite element analysis. To make an in-depth examination into analytical accuracy of the proposed method, this study considers a tank subjected to the harmonic base excitation whose driving period is identical with the natural period of the tank bulging motion. It may allow the straightforward application of a magnification factor of the SDOF oscillator subjected to the harmonic base excitation to evaluating the response of the tank bulging motion. In addition, since out-of-round deformation of the tank shell enlarges the uplift displacement of tanks [7], this study employs a numerical tank whose cylindrical shell has multistage stiffeners modeled by a rigid element. The comparison reveals that the proposed method may approximate the angular acceleration accompanying the tank rocking motion if de-amplification of the tank rocking motion due to impact between the tank bottom plate and the foundation is properly taken into account.

Here, the proposed method is insufficient for evaluating the tank response quantities accompanying the tank rocking motion in a present form, because the relationship between the angular acceleration accompanying the tank rocking motion and deformation of the tank bottom plate is still unknown. However it is worth exploring how the proposed method accurately predicts the tank rocking motion based on the knowledge of dynamical mechanism given to date. Moreover, this study ignores effects of sloshing on the tank rocking motion, because the lateral force induced by sloshing is small comparing to that induced by bulging. In addition, the previous shaker table tests [8] and numerical analyses [9] revealed that significant sloshing waves were not observed during the tank rocking motion, because the natural period of sloshing is naturally apart from that of the tank bulging motion that dominates the tank rocking motion and their maxima do not coincide.

2. Equations of motion of 2DOF model

Consider a 2DOF system consisting of a Spring-Mass (SM) system and another mass attached to its bottom (hereafter 2DOF model). Figure 1 gives its geometry. m_1 and k represents a value of mass of the vibrant mass and the spring constant of the SM system of the 2DOF model, respectively. A value of mass of the lower mass is m_2. The SM system begins to vibrate at the initiation of the ground motion, while the 2DOF model commences to rock when the Overturning Moment (OM) induced by the SM system of the 2DOF model overcomes the Restoring Moment (RM) inherent in the 2DOF model. Set the origin of the global coordinates *X-Y* and that of the element coordinates *x-y* at the left bottom edge of the 2DOF model (See a point “0” in Fig.1). Consider that the vibrant mass of the SM system displaces x_1 and the 2DOF model rotates θ pivoting at the left bottom edge from their initial positions, respectively. Here, the displacement x_1 is measured on the inclined element coordinates *x-y*, while the rotational angle θ is measured on the global coordinates *X-Y*. Taking the moment inertia I_1 of the vibrant mass m_1 and that I_2 of the lower mass m_2 into account, Lagrangian of 2DOF model is given as;

$$\begin{aligned} L = {} & \frac{1}{2} m_1 \left\{ \dot{x}_1^2 + x_1^2 \dot{\theta}^2 + 2 x_1 R_1 \dot{\theta}^2 \sin\alpha_1 - 2 \dot{x}_1 R_1 \dot{\theta} \cos\alpha_1 \right\} + \frac{1}{2} \left\{ I_1 + m_1 R_1^2 \right\} \dot{\theta}^2 - m_1 g \left\{ R_1 \cos(\alpha_1 - \theta) + \sin\theta x_1 - R_1 \cos\alpha_1 \right\} \\ & + \frac{1}{2} \left\{ I_2 + m_2 R_2^2 \right\} \dot{\theta}^2 - m_2 g \left\{ R_2 \cos(\alpha_2 - \theta) - R_2 \cos\alpha_2 \right\} - \frac{1}{2} k x_1^2 \end{aligned} \tag{1}$$

The equation of motion for translational motion of the vibrant mass of the SM system of the 2DOF model is derived as;

$$m_1\ddot{x}_1 - m_1 R_1 \ddot{\theta}\cos\alpha_1 + m_1 g\sin\theta - m_1\left(x_1 + R_1\sin\alpha_1\right)\dot{\theta}^2 + kx_1 + m_1\ddot{z}_H\cos\theta = 0 \tag{2}$$

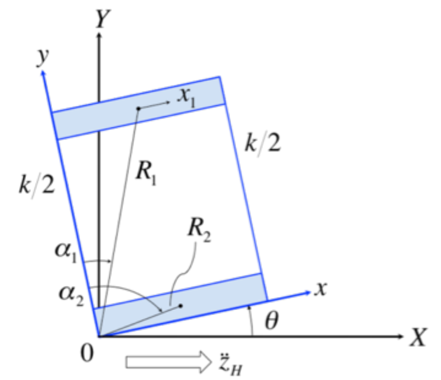

Fig. 1 – 2DOF model in displaced and rotated position

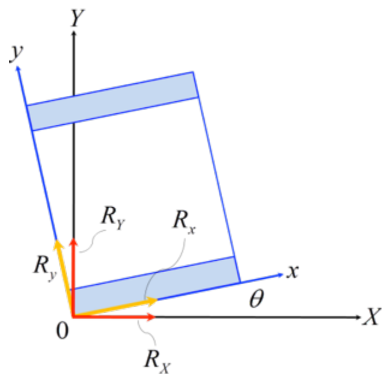

Fig. 2 – Base shear and reaction of 2DOF model

Here, to simplify notation of Eq. (2), the damping term of the SM system of the 2DOF model is not explicitly shown. However, this study assumes that the damping effects on the response of the SM system of the 2DOF model are naturally included by giving the response of the SM system by response acceleration spectra discussed later. The equation of motion for the rocking motion of the 2DOF model is also derived as;

$$\begin{aligned}&\left\{m_1\left(x_1^2 + 2x_1R_1\sin\alpha_1 + R_1^2\right) + I_1 + I_2 + m_2R_2^2\right\}\ddot{\theta} - m_1\ddot{x}_1R_1\cos\alpha_1 + 2m_1\dot{x}_1\dot{\theta}\left(x_1 + R_1\sin\alpha_1\right) + m_1g\left\{R_1\sin\left(\alpha_1 - \theta\right) + x_1\cos\theta\right\}\\ &+ m_2gR_2\sin\left(\alpha_2 - \theta\right) - \left[m_1\left\{R_1\cos\left(\alpha_1 - \theta\right) + x_1\sin\theta\right\} + m_2R_2\cos\left(\alpha_2 - \theta\right)\right]\ddot{z}_H = 0\end{aligned} \tag{3}$$

The condition to initiate the rocking motion of the 2DOF model is given by $RM<OM$. RM and OM are given as;

$$RM = (m_1R_1\sin\alpha_1 + m_2R_2\sin\alpha_2)g,\quad OM = m_1R_1\cos\alpha_1\left(\ddot{x}_1 + \ddot{z}_H\right) + m_2R_2\cos\alpha_2\ddot{z}_H \tag{4}$$

Moreover, from the equilibrium among translational and rotational forces on the inclined element coordinates, R_x and R_y are defined as forces to support rotation of the 2DOF model pivoting at the left bottom edge of the lower mass. (See Fig. 2) Then transform them into the global coordinates, the base shear R_X and reaction R_Y at the pivoting left bottom edge of the lower mass are derived as;

$$\begin{aligned}R_X =\ & m_1g\sin2\theta - m_1R_1\dot{\theta}^2\sin\left(\alpha_1 + \theta\right) - m_1R_1\ddot{\theta}\cos\left(\alpha_1 + \theta\right) - m_1x_1\dot{\theta}^2\cos\theta + m_1x_1\ddot{\theta}\sin\theta + 2m_1\dot{x}_1\dot{\theta}\sin\theta + m_1\ddot{z}_H\cos2\theta\\ &+ m_1\ddot{x}_1\cos\theta + m_2g\sin2\theta - m_2R_2\dot{\theta}^2\sin\left(\alpha_2 + \theta\right) - m_2R_2\ddot{\theta}\cos\left(\alpha_2 + \theta\right) + m_2\ddot{z}_H\cos2\theta\end{aligned} \tag{5a}$$

$$\begin{aligned}R_Y =\ & m_1g\cos2\theta - m_1R_1\dot{\theta}^2\cos\left(\alpha_1 + \theta\right) + m_1R_1\ddot{\theta}\sin\left(\alpha_1 + \theta\right) + m_1x_1\dot{\theta}^2\sin\theta + m_1x_1\ddot{\theta}\cos\theta + 2m_1\dot{x}_1\dot{\theta}\cos\theta - m_1\ddot{z}_H\sin2\theta\\ &- m_1\ddot{x}_1\sin\theta + m_2g\cos2\theta - m_2R_2\dot{\theta}^2\cos\left(\alpha_2 + \theta\right) + m_2R_2\ddot{\theta}\sin\left(\alpha_2 + \theta\right) - m_2\ddot{z}_H\sin2\theta\end{aligned} \tag{5b}$$

3. Equations of motion of evaluating tank rocking motion

The equations of motion for the 2DOF model are converted into those of the tank rocking motion by replacing physical quantities of the 2DOF model for corresponding ones specifying the tank rocking motion based on mechanical analogy. First, the SM system of the 2DOF model is regarded as the tank bulging system. The vibrant mass of the SM system is replaced by the effective mass of fluid for bulging motion m_b, while that of the spring constant is adjusted to match the natural period of the tank bulging motion. Unlike the vibrant mass of the SM system of the 2DOF model, the effective mass of fluid for bulging motion m_b partially contributes to the tank rocking motion through the effective mass of fluid for rocking-bulging interaction m_{rb}. Contrary, the effective mass of fluid for rocking motion m_r and its moment inertia I_r about either pivoting bottom edge dominate the tank rocking motion. In Ref. [6], these effective masses of fluid are defined by solving boundary value problem for the motion of fluid induced by the tank rocking and/or bulging motions. Values of m_b, m_r and

m_{rb} are a function of the aspect of tank, while values of m_r and m_{rb} are a function of the ratio of the uplift width of the tank bottom plate to the diameter of the tank in addition to the aspect of tank. Therefore, the terms in Eqs. (2) and (3) specifying the action of rotational forces are replaced by m_r, while those giving the interaction between translational and rotational motions are replaced by m_{rb}. The masses of the shell m_{sh}, roof m_{rf}, and an un-uplift part of the bottom plate m_{bpUL} are also included in a priori. Here, the uplift and un-uplift parts of the tank bottom plate are distinguished. Figure 3 shows an analytical model of the tank rocking motion.

The equation of motion for the tank bulging motion is rewritten as;

$$m_b\ddot{x}_1 - m_{rb}R_{rb}\ddot{\theta}\cos\alpha_{rb} + m_b g\sin\theta - m_{rb}\left(x_1 + R_{rb}\sin\alpha_{rb}\right)\dot{\theta}^2 + kx_1 + m_b\ddot{z}_H\cos\theta = 0 \tag{6}$$

The equation of motion for the tank rocking motion is rewritten as;

$$\begin{aligned}&\left\{m_{rb}(x_1^2 + 2x_1R_{rb}\sin\alpha_{rb}) + \left(I_{rf} + I_{sh} + I_{bpUL} + I_r\right) + \left(m_{rf}R_{rf}^2 + m_{sh}R_{sh}^2 + m_{bpUL}R_{bpUL}^2 + m_rR_r^2\right)\right\}\ddot{\theta} - m_b\ddot{x}_1R_b\cos\alpha_b \\ &+ 2m_{rb}\dot{x}_1\dot{\theta}\left(x_1 + R_{rb}\sin\alpha_{rb}\right) + \left\{m_{rf}R_{rf}\sin\left(\alpha_{rf} - \theta\right) + m_{sh}R_{sh}\sin\left(\alpha_{sh} - \theta\right) + m_{bpUL}R_{bpUL}\sin\left(\alpha_{bpUL} - \theta\right) + m_rR_r\sin\left(\alpha_r - \theta\right)\right\}g \\ &- \left[m_b\left\{R_b\cos\left(\alpha_b - \theta\right) + x_1\sin\theta\right\}\right]\ddot{z}_H - \left\{m_{rf}R_{rf}\cos\left(\alpha_{rf} - \theta\right) + m_{sh}R_{sh}\cos\left(\alpha_{sh} - \theta\right) + m_{bpUL}R_{bpUL}\cos\left(\alpha_{bpUL} - \theta\right)\right\}\ddot{z}_H = 0\end{aligned} \tag{7}$$

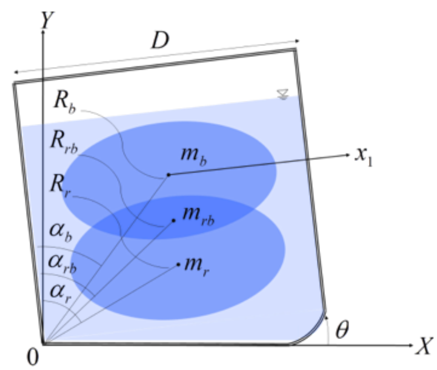

Fig. 3 – Analytical model of tank rocking motion

This study ignores responses of the shell and roof and assumes that the tank bottom plate is on the ground at the initiation of the tank rock motion. (See Fig. 4) Therefore, the *RM* and *OM* are rewritten as;

$$RM = (m_{rf} + m_{sh})Dg/2\,,\quad OM = m_bH_b\left(\ddot{x}_1 + \ddot{z}_H\right) + (m_{rf}H_{rf} + m_{sh}H_{sh})\ddot{z}_H \tag{8}$$

Follow the manner in deriving Eqs. (6) and (7), the base shear R_X and reaction R_Y during the tank rock motion (See Fig. 5) are also rewritten as;

$$\begin{aligned}R_X =\ & m_bg\sin 2\theta - m_{rb}R_{rb}\dot{\theta}^2\sin\left(\alpha_{rb} + \theta\right) - m_{rb}R_{rb}\ddot{\theta}\cos\left(\alpha_{rb} + \theta\right) + m_b\ddot{z}_H\cos 2\theta + m_b\ddot{x}_1\cos\theta \\ &+ (m_{rf} + m_{sh} + m_{bpUL} + m_{bpNUL})\cdot\left\{g\sin 2\theta + \ddot{z}_H\cos 2\theta\right\} + m_{rb}\left(2\dot{x}_1\dot{\theta}\sin\theta + x_1\ddot{\theta}\sin\theta - x_1\dot{\theta}^2\cos\theta\right) \\ &- \left(m_{rf}R_{rf}\cos\alpha_{rf} + m_{sh}R_{sh}\cos\alpha_{sh} + m_{bpUL}R_{bpUL}\cos\alpha_{bpUL} + m_rR_r\cos\alpha_r\right)\left(\ddot{\theta}\cos\theta + \dot{\theta}^2\sin\theta\right) \\ &+ \left(m_{rf}R_{rf}\sin\alpha_{rf} + m_{sh}R_{sh}\sin\alpha_{sh} + m_{bpUL}R_{bpUL}\sin\alpha_{bpUL} + m_rR_r\sin\alpha_r\right)\left(\ddot{\theta}\sin\theta - \dot{\theta}^2\cos\theta\right)\end{aligned} \tag{9a}$$

$$\begin{aligned}R_Y =\ & m_bg\cos 2\theta - m_{rb}R_{rb}\dot{\theta}^2\cos\left(\alpha_{rb} + \theta\right) + m_{rb}R_{rb}\ddot{\theta}\sin\left(\alpha_{rb} + \theta\right) - m_b\ddot{z}_H\sin 2\theta - m_b\ddot{x}_1\sin\theta \\ &+ (m_{rf} + m_{sh} + m_{bpUL} + m_{bpNUL})\left\{g\cos 2\theta - \ddot{z}_H\sin 2\theta\right\} + m_{rb}\left(2\dot{x}_1\dot{\theta}\cos\theta + x_1\ddot{\theta}\cos\theta + x_1\dot{\theta}^2\sin\theta\right) \\ &+ \left(m_{rf}R_{rf}\cos\alpha_{rf} + m_{sh}R_{sh}\cos\alpha_{sh} + m_{bpUL}R_{bpUL}\cos\alpha_{bpUL} + m_rR_r\cos\alpha_r\right)\left(\ddot{\theta}\sin\theta - \dot{\theta}^2\cos\theta\right) \\ &+ \left(m_{rf}R_{rf}\sin\alpha_{rf} + m_{sh}R_{sh}\sin\alpha_{sh} + m_{bpUL}R_{bpUL}\sin\alpha_{bpUL} + m_rR_r\sin\alpha_r\right)\left(\ddot{\theta}\cos\theta + \dot{\theta}^2\sin\theta\right) + \left(m_l - m_b\right)g\end{aligned} \tag{9b}$$

The last term of Eq. (9b) is added to maintain the total weight of fluid, because the effective mass of fluid for bulging motion is a part of the mass of fluid fulfilled in the tank that only responds to the horizontal base acceleration.

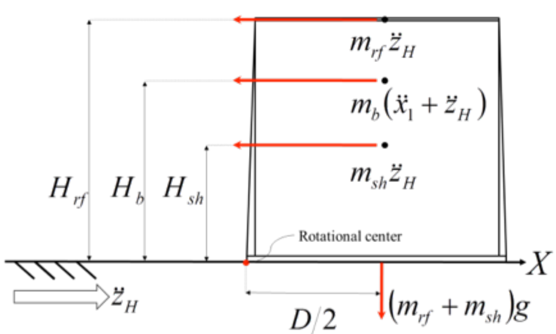

Fig. 4 – Forces at the initiation of the tank rocking motion

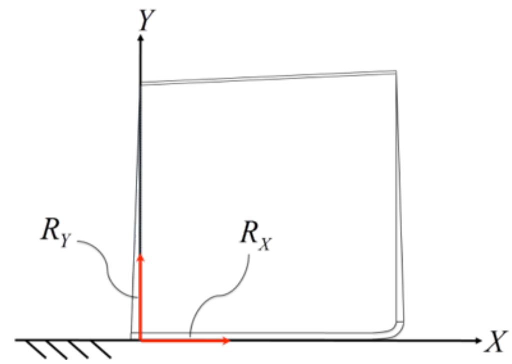

Fig. 5 – Base shear and reaction during the tank rocking motion

4. Simplified analysis of tank rocking motion

In the absence of uplift, the product of the maximum ground acceleration $\left(\ddot{z}_H\right)_{\max}$ and the ratio of response acceleration to the maximum ground acceleration $S_{AH}^{ratio}\left(T_b,h_b\right)$ may determine the maximum response of the tank bulging motion. T_b and h_b are the natural period of the tank bulging motion and its damping ratio, respectively. Eqs. (6) and (7) are rearranged to give the maximum response of the tank bulging motion by the response acceleration spectrum and simplified by ignoring some terms according to their effects on the response of interest. It implies that the proposed method calculates the tank rocking motion at the instant of the maximum tank bulging motion. Moreover, since fluid pressure accompanying the tank rock motion is given as a function of the angular acceleration [6], this study aims to derive a concise and easy method of evaluating the angular acceleration that is indispensable in designing the tank with adequate safety margin.

A value of response spectra gives the absolute maximum response acceleration of the tank bulging system $\left(x_1+\ddot{z}_H\right)_{\max}$ which naturally includes damping effects.

$$\left(\ddot{x}_1+\ddot{z}_H\right)_{\max}=S_{AH}^{ratio}\left(T_b,h_b\right)\left(\ddot{z}_H\right)_{\max} \tag{10}$$

From Eqs. (8) and (10), the overturning moment is readily calculated as;

$$OM=m_bH_bS_{AH}^{ratio}\left(T_b,h_b\right)\left(\ddot{z}_H\right)_{\max}+\left(m_{rf}H_{rf}+m_{sh}H_{sh}\right)\left(\ddot{z}_H\right)_{\max} \tag{11}$$

Substitution of Eq.(11) into Eq.(8) gives the maximum ground acceleration required to initiate the tank rocking motion.

$$\left(\ddot{z}_H\right)_{\max}>\frac{\left(m_{rf}+m_{sh}\right)Dg}{2\left\{m_bH_bS_{AH}^{ratio}\left(T_b,h_b\right)+\left(m_{rf}H_{rf}+m_{sh}H_{sh}\right)\right\}} \tag{12}$$

In contrast, the uplift height of the tank bottom plate is presumed to be up to 1 meter in the tank with a diameter of 30 meters. Therefore, the rotational angle of the tank θ is about 1/30 radian and a value of trigonometric function are regarded as $\sin\theta=0.03\cong 0$ and $\cos\theta=0.999\cong 1$. Since a value of the angular velocity $\dot{\theta}$ seems to be small compering to that of the angular acceleration $\ddot{\theta}$, the terms of centrifugal force and Coriolis force are reasonably eliminated. Substituting them into Eq. (6), the equation of motion for tank bulging motion is simplified as;

$$m_b S_{AH}^{ratio}(T_b, h_b)(\ddot{z}_H)_{\max} - m_{rb} H_{rb} \ddot{\theta} + k x_1 = 0 \tag{13}$$

Here, the notation $H_{rb} = R_{rb} \cos\alpha_{rb}$ is used to simplify notation. Moreover, since the uplift width of the tank bottom plate is up to 6 to 7 percent of the diameter of tank [2], contribution of inertia forces arising from the uplift part of the tank bottom plate to the tank rock motion is negligible. The rotational inertia force induced by the effective mass of fluid for rocking-bulging interaction $m_{rb} x_1^2 \ddot{\theta}$ is negligible, because displacement of the tank bulging system x_1 is relatively small comparing to the diameter of the tank. Therefore, equation of motion for tank rocking motion given by Eq. (7) is also simplified as;

$$\begin{aligned} &\left\{m_{rb} x_1 D + (I_{rf} + I_{sh} + I_r) + (m_{rf} R_{rf}^2 + m_{sh} R_{sh}^2 + m_r R_r^2)\right\}\ddot{\theta} - m_b H_b S_{AH}^{ratio}(T_b, h_b)(\ddot{z}_H)_{\max} \\ &\quad + (m_{rf} + m_{sh} + m_r) g D/2 - (m_{rf} H_{rf} + m_{sh} H_{sh})(\ddot{z}_H)_{\max} = 0 \end{aligned} \tag{14}$$

Here, the notation $H_b = R_b \cos\alpha_b$, $H_r = R_r \cos\alpha_r$, $H_{rf} = R_{rf} \cos\alpha_{rf}$, $H_{sh} = R_{sh} \cos\alpha_{sh}$ are used. In addition, $R_r \sin\alpha_r \cong D/2$ and $R_{rb} \sin\alpha_{rb} \cong D/2$ are assumed for simplification.

Equations (13) and (14) are simultaneous equations with respect to the angular acceleration $\ddot{\theta}$. Give the spring constant of the tank bulging system with the effective mass of fluid for bulging motion and the natural period of the tank bulging system $k = 4\pi^2 m_b / T_b^2$, and solve the simultaneous equations for $\ddot{\theta}$.

$$\begin{aligned} &\frac{D H_{rb} m_{rb}^2 T_b^2}{4\pi^2 m_{\mathbf{b}}} \ddot{\theta}^2 + \left[(I_{rf} + I_{sh} + I_r) + (m_{rf} R_{rf}^2 + m_{sh} R_{sh}^2 + m_r R_r^2) - \frac{D m_{rb} T_b^2}{4\pi^2} S_{AH}^{ratio}(T_b, h_b)(\ddot{z}_H)_{\max}\right]\ddot{\theta} \\ &\quad + (m_{rf} + m_{sh} + m_r) g D/2 - \left\{m_b H_b S_{AH}^{ratio}(T_b, h) + (m_{rf} H_{rf} + m_{sh} H_{sh})\right\}(\ddot{z}_H)_{\max} = 0 \end{aligned} \tag{15}$$

Equation (15) is a quadratic equation in terms of $\ddot{\theta}$, and a value of the angular acceleration $\ddot{\theta}$ representing the tank rock motion is readily calculated as;

$$\begin{aligned} &\ddot{\theta} = \frac{1}{2C_A}\left(-C_B + \sqrt{C_B^2 - 4C_A C_C}\right) \\ &C_A = \frac{D H_{rb} m_{rb}^2 T_b^2}{4\pi^2 m_{\mathbf{b}}},\ C_B = (I_{rf} + I_{sh} + I_r) + (m_{rf} R_{rf}^2 + m_{sh} R_{sh}^2 + m_r R_r^2) - \frac{D m_{rb} T_b^2}{4\pi^2} S_{AH}^{ratio}(T_b, h_b)(\ddot{z}_H)_{\max}, \\ &C_C = (m_{rf} + m_{sh} + m_r) g D/2 - \left\{m_b H_b S_{AH}^{ratio}(T_b, h_b) + (m_{rf} H_{rf} + m_{sh} H_{sh})\right\}(\ddot{z}_H)_{\max} \end{aligned} \tag{16}$$

In contrast, in the absence of the tank rock motion, the equation of motion for the tank bulging system is readily given as;

$$m_b(\ddot{x}_1 + \ddot{z}_H) + k x_1 = 0 \tag{17}$$

Substitution of Eq. (17) into Eq. (13) yields the absolute response acceleration representing the tank bulging motion $(\ddot{x}_1 + \ddot{z}_h)$ that includes the rocking-bulging interaction effects.

$$(\ddot{x}_1 + \ddot{z}_h) = \left\{S_{AH}^{ratio}(T_b, h_b)(\ddot{z}_H)_{\max}\right\} - \frac{m_{rb}}{m_b} H_{rb} \ddot{\theta} \tag{18}$$

As the second term of the right hand side of Eq. (18) shows, the tank rocking motion reduces the tank bulging response due to the rocking-bulging interaction. In addition, Eq. (18) naturally gives the tank bulging response in the absence of the tank rocking motion. Similarly, the base shear R_X and reaction R_Y during the tank rocking motion are also simplified as;

$$R_X = m_b(\ddot{x}_1 + \ddot{z}_h) + (m_{rf} + m_{sh} + m_{bp})(\ddot{z}_H)_{\max} - (m_{rb}H_{rb} + m_{rf}H_{rf} + m_{sh}H_{sh} + m_r H_r)\ddot{\theta} \tag{19a}$$

$$R_Y = (m_l + m_{rf} + m_{sh} + m_{bp})g + (m_{rb} + m_{rf} + m_{sh} + m_r)\frac{D}{2}\ddot{\theta} \tag{19b}$$

Since the tank rocking motion counteracts the tank bulging motion, the base shear is reduced when the tank rocks. The third term of the right hand side of Eq. (19a) gives its effects accompanying the tank rocking motion and rocking-bulging interaction. Employing Eq. (18), Eq. (19a) naturally gives the base shear induced by the tank bulging response in the absence of the tank rocking motion. In contrast, Eq. (19b) naturally becomes the total weight of the tank in the absence of the tank rocking motion. Being contrary to the base shear, the reaction increases when the tank bottom plate is going up, while that decreases when the tank bottom plate is going down. It is consistent with self-weight lightening effects inferred from the reaction of a rocking rectangular rigid block [10] and free rocking experiments of the rectangular rigid body and tank [11]. Since Eq. (16) gives a positive value of $\ddot{\theta}$, use it for verifying the bearing capacity of the tank foundation, while use the opposite of it for verifying the commencement of tank slip [12] and walking [13] in design process.

5. Accuracy of the simplified calculation

The angular acceleration accompanying the tank rocking motion calculated by the proposed method is compared with that computed by the explicit finite element analysis. To make an in-depth examination into analytical accuracy of the proposed method, this study considers an unanchored tank set on the almost rigid foundation subjected to the harmonic base excitation whose driving period is identical with the natural period of the tank bulging motion. It may allow the straightforward application of a magnification factor of response acceleration of the SDOF oscillator subjected to the harmonic base excitation according to the number of waves experienced to evaluating the response of the tank bulging motion. In addition, since the proposed method does not take account of out-of-round deformation of the cylindrical shell, the numerical tank model with the undeformable cylindrical shell is used. Although Nakashima [7] pointed out that the out-of-round deformation of the cylindrical shell enlarges the uplift displacement of tanks, taking such effects into account remains as future work.

A cylindrical shell flat-bottom tank without a roof whose shell height and diameter are 30.0 m and 51.5 m is considered. Symmetry of tank's behavior with respect to an input axis of the horizontal base excitation enables to use a half-part of the tank model (See Fig. 6a). A cylindrical shell consists of aluminum alloy plates that have 16.0 mm to 54.5 mm in thickness. A tank bottom plate has 6.0 mm in thickness while the annular plate whose width is 4.0 m has 32.7 mm in thickness. The cylindrical shell and bottom plate are modelled by shell elements consisting of 21,639 nodes and 21,640 elements (See Fig. 6b). The density, elastic modulus and Poisson's ratio and of aluminum alloy are 2.670x10^{-6} kg/mm^3, 70000N/mm^2 and 0.3, respectively. The tank stores liquefied natural gas (LNG) whose density is 0.47 t/m^3 and its depth is 28.824 m. The fluid is modelled by Euler elements consisting of 301,168 nodes and 301,400 elements (See Fig. 6c). Viscosity of fluid is assumed to be 1.00 x10^{-20}. In modeling fluid, this study employs Arbitrary Lagrangian Eulerian (ALE) method for satisfactory results. The conventional calculation of the first natural period of the tank bulging motion [14] suggests 0.4 seconds. The numerical model also has an almost rigid foundation 70 m in diameter and 10 m in thickness and is modelled by solid elements consisting of 15,651 nodes and 10,640 elements (See Fig. 6d). Its density, elastic modulus and Poisson's ratio are 7.700 x10^{-6} kg/mm^3, 30000 N/mm^2 and 0.3, respectively.

For simulating the rocking motion of the undeformable cylindrical shell tank, the multistage rigid stiffeners modeled by rigid elements are attached to the cylindrical shell at an interval of 1 meter to prevent its out-of-round deformation. In addition, the relative displacement between the tank bottom plate and foundation is constrained to prevent the un-uplift part of the tank bottom plate from sliding on the foundation partially. Ref. [15] shows its validity in stabilizing the numerical analysis. Applying 1% structural damping ratio and the horizontal sinusoidal base excitation whose driving period and amplitude are 0.4 second and 1000 mm/s^2 respectively, a time history of the tank response is computed by the explicit finite element analysis.

Figure 7a shows a time history of the uplift displacement of the left and right side edges of the tank bottom plate. The node number 4895 represents the right bottom edge, while the node number 4735 does the left bottom edge (See also Fig. 6b). In the time history analyses, the first one second is used to increase gravitational acceleration gradually for taking the dead weight of the tank into account. Therefore, the horizontal sinusoidal base acceleration begins at one second and lasts four seconds (See a green solid line in Fig. 7a). The left and right bottom edge uplifts reciprocally and marks almost the same uplift displacement in turn. This is evidence that the tank harmonically rocks. Figure 7b depicts distribution of the uplift displacement of the tank bottom plate along diameter at 2.3 seconds. The uplift width of the tank bottom plate is 2560 mm that reaches 4.7 % of the tank diameter.

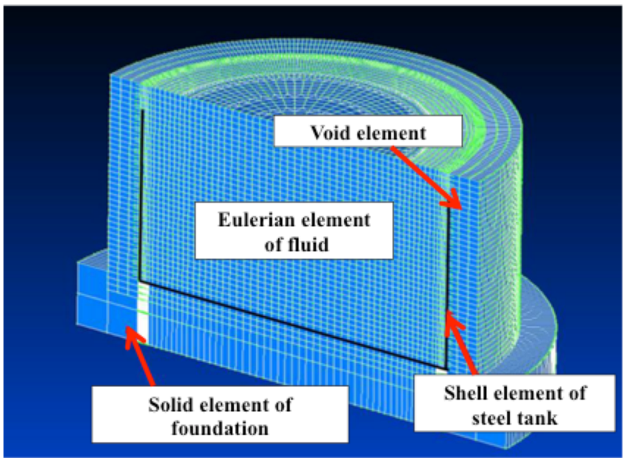

Fig. 6a – Numerical tank modeled in LS-DYNA

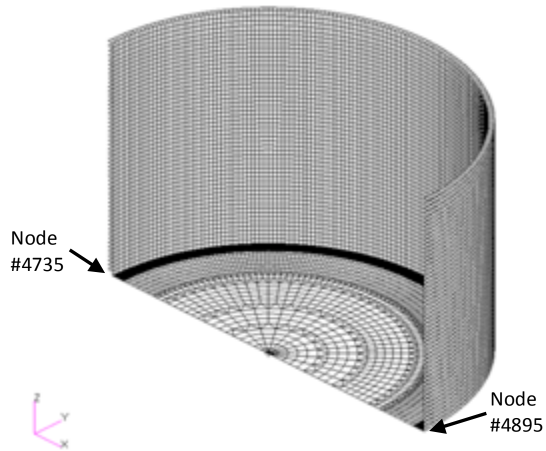

Fig. 6b – Numerical model of shell and bottom plate

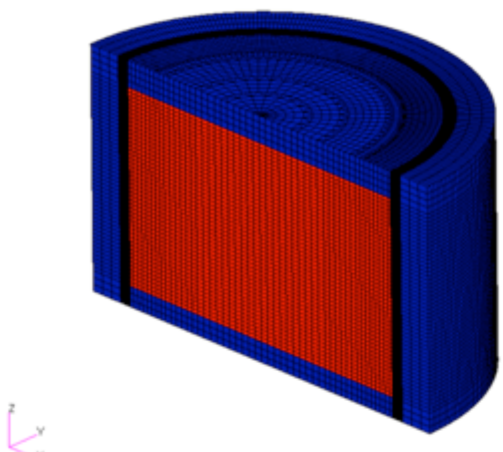
Fig. 6c – Numerical model of fluid

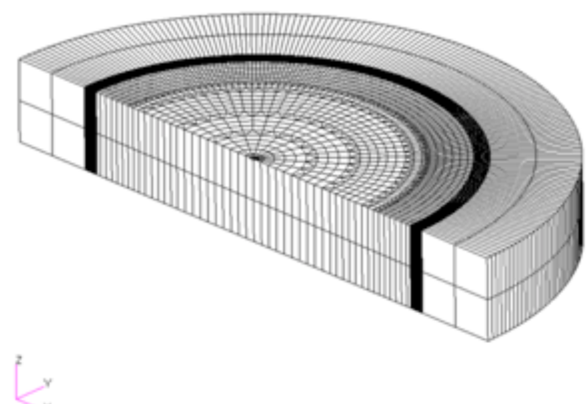
Fig. 6d – Numerical model of foundation

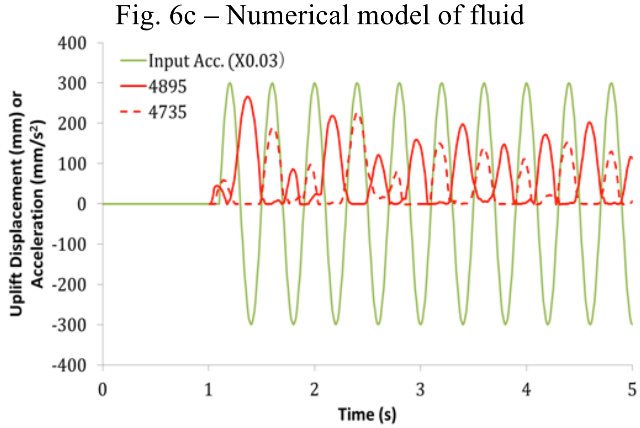

Fig. 7a – Input acceleration and uplift displacement

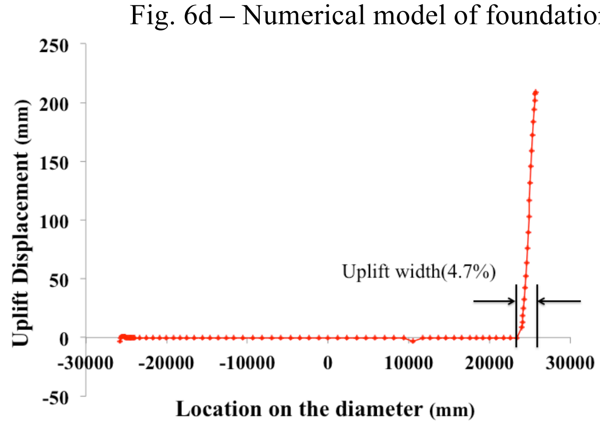

Fig. 7b – Uplift width of the tank bottom plate (t = 2.3s)

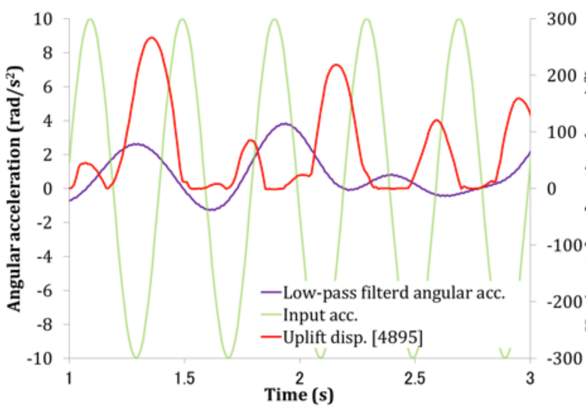

Fig. 8 – Angular acceleration and uplift displacement

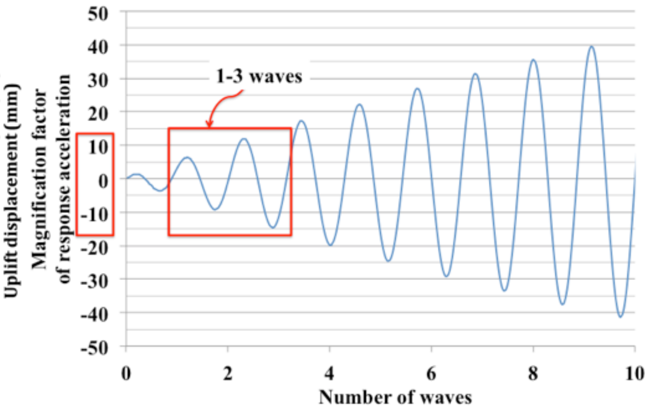

Fig. 9 – Magnification factor (h_b=0.01)

Figure 8 shows an enlarged view of a time history (1-3 seconds) of the angular acceleration of the right bottom edge accompanying the tank rock motion and the uplift displacement of that. Since an original time history of the angular acceleration includes impulses accompanying landing of the tank bottom plate on the foundation, the time history of the angular acceleration shown on Fig. 8 is passed through a 3 Hz low-pass filter (See a violet solid line on Fig. 8). Since effects of impulses extend as the number of landing increases, this study focuses on the angular acceleration observed at the first few landing. Therefore, this study picks up 2.5-4.0 rad/s^2 as a representative value of the angular acceleration computed (See about 1.3 and 2 seconds on Fig. 8). In contrast, Fig. 9 shows a development history of a magnification factor of response acceleration of the SDOF oscillator subjected to the harmonic base excitation that possesses 1% damping ratio with respect to the number of waves. In Fig. 8, since the first few landing is observed at the interval between the first and the third horizontal sinusoidal wave input, this study uses 5 to 15 as a value of the magnification factor corresponding to it (See Fig. 9).

Table 1 – Dynamical properties used in the simplified calculation

	Uplift width (3%)	Uplift width (4%)	Uplift width (5%)
H_{rb} (m) [5]	12.012	11.911	11.807
I_r (kg m^4) [5]	823.787 x 10^6	885.284 x 10^6	944.754 x 10^6
m_b (kg) [11]	1.787 x 10^7		
m_{rb} (kg) [5]	3.467 x 10^6	3.706 x 10^6	3899398
m_r (kg) [5]	5.101 x 10^6	5.418 x 10^6	5677616
h_b	0.01		
T_b (seconds)	0.4		
$S_{AH}^{ratio}(T_b, h_b)$	5 to 15		
$(\ddot{z}_H)_{\max}$ (m/s^2)	10.0		

In contrast, assuming 3-5% of the ratio of the uplift width to diameter of the tank bottom plate, Table 1 calculates values of physical quantities of the 2DOF model corresponding to the numerical tank model depicted on Fig. 6. Table 2a and 2b summarizes results of the angular acceleration calculated by Eq. (16). Here, the term $S_{AH}^{ratio}(T_b, h_b)$ employs the value of the magnification factor. Results of Table 2a include the dead weight of the tank, while those of table 2b exclude that. Since their discrepancies are 10 % and more, ignoring the dead weight of the tank in evaluating the angular acceleration may yield erroneous results. Meanwhile from Fig. 7a, the uplift displacement induced by the second horizontal sinusoidal wave may represent them, because almost the same uplift displacement appears in turn after that. Therefore, the magnification factor due to the second wave is reasonably assumed as 10-11 form Fig. 9, while the ratio of the uplift width is reasonably assumed as 4-5% from Fig. 7b. These presumptions yield 3.0-3.5 rad/s^2 as a representative value of the angular acceleration calculated by Eq. (16) from Tab. 2b. The value of the angular acceleration calculated (3.0-3.5 rad/s^2) is in good agreement with that computed (2.5-4.0 rad/s^2), although it does not include de-amplification of the angular acceleration due to restitution accompanying landing of the tank bottom plate on the foundation. Here, an actual value of the coefficient of restitution between the tank bottom plate and the foundation has not been known. If we assume it to be 0.7 and one or two times restitution between the tank bottom plate and the foundation, the angular acceleration is reduced to 0.7 (=0.7^1) or 0.49 (=0.7^2) times and then we will have 2.45 rad/s^2 or 1.72 rad/s^2 as the value of the angular acceleration calculated. They seem to be slightly smaller than the angular acceleration computed. It suggests that inclusion of de-amplification effects on the proposed method remains as future work.

Table 2a – Calculation results of the angular acceleration (tank dead weight is included)

$S_{AH}^{ratio}(T_b, h_b)$	$\ddot{\theta}$ (rad/s^2)		
	Uplift width (3%)	Uplift width (4%)	Uplift width (5%)
5	1.590	1.497	1.426
6	1.956	1.844	1.759
7	2.321	2.191	2.092
8	2.688	2.539	2.426
9	3.056	2.888	2.761
10	3.424	3.238	3.097
11	3.793	3.589	3.433
12	4.164	3.940	3.770
13	4.534	4.292	4.108
14	4.906	4.645	4.447
15	5.279	4.999	4.786

Table 2b – Calculation results of the angular acceleration (the tank dead weight is excluded)

$S_{AH}^{ratio}(T_b, h_b)$	$\ddot{\theta}$ (rad/s^2)					
	Uplift width (3%)	Discrepancy [%]	Uplift width (4%)	Discrepancy [%]	Uplift width (5%)	Discrepancy [%]
5	1.805	13.5	1.688	12.8	1.600	12.2
6	2.218	13.4	2.077	12.7	1.972	12.1
7	2.631	13.3	2.467	12.6	2.344	12.0
8	3.046	13.3	2.858	12.6	2.717	12.0
9	3.462	13.3	3.250	12.5	3.092	12.0
10	3.878	13.3	3.644	12.5	3.467	12.0
11	4.296	13.3	4.038	12.5	3.843	11.9
12	4.715	13.2	4.433	12.5	4.220	11.9
13	5.135	13.2	4.829	12.5	4.598	11.9
14	5.556	13.2	5.226	12.5	4.977	11.9
15	5.978	13.2	5.624	12.5	5.357	11.9

6. Conclusion

Based on mechanical analogy between the rocking motion of the 2DOF model and that of the cylindrical tanks, the equations of motion for the tank bulging motion, that for the tank rocking motion, the base shear and reaction are derived. The equations of motion are simplified by ordering some terms and employing the value of response acceleration spectrum. The proposed method is given in a closed form that explicitly includes effects of the rocking-bulging interaction and can calculate the angular acceleration accompanying the tank rocking motion. Employing the undeformable cylindrical shell tank subjected to the horizontal sinusoidal wave, the angular acceleration calculated by the proposed method is compared with that computed by the explicit finite element analysis. Comparison reveals that ignorance of the dead weight in evaluating the angular acceleration may yield erroneous results and the proposed method may give a reasonable value of the angular acceleration. However, since the proposed method does not take account of 1) de-amplification of the angular acceleration due to restitution accompanying landing of the tank bottom plate on the foundation and 2) enlargement of uplift displacement due to out-of-round deformation of the cylindrical shell of the tank, their inclusion on the proposed method remains as future work.

7. Acknowledgements

A part of this research was supported by JSPS KAKENHI Grant Number 21560242. This support is gratefully acknowledged.

8. Nomenclature

For 2DOF Model

k : Spring constant

m_1 : Mass of the Spring-Mass System (SMS)

m_2 : Mass of the mass attached to the base of the SMS

R_1 : Length between origin *O* and gravity center of m_1

R_2 : Length between origin *O* and gravity center of m_2

x_1 : Displacement of m_1

$\ddot{z}_H$: Horizontal ground acceleration

α_1 : Angle between vertical line y and R_1

α_2 : Angle between vertical line y and R_2

θ : Rotational angle of 2DOF model

For Tank Model

D : Diameter of the cylindrical tank.

H_{rf} : Height of the gravity center of m_{rf}

H_{rb} : Height of the gravity center of m_{rb}

H_{sh} : Height of the gravity center of m_{sh}

I_{bpUL} : Moment of inertia of m_{bpUL} at the gravity center

I_{bpNUL} : Moment of inertia of m_{bpNUL} at the gravity center

I_{rf} : Moment of inertia of m_{rf} at the gravity center

I_{sh} : Moment of inertia of m_{sh} at the gravity center

I_r : Moment of inertia of m_r at the gravity center

m_b : Effective mass of fluid for bulging motion

m_{rb} : Effective mass of fluid for rocking-bulging interaction

m_{bp} : Mass of tank bottom plate

m_{bpUL} : Mass of tank bottom pale where uplifts

m_{bpNUL} : Mass of tank bottom plate where does not uplift

m_l : Mass of fluid fulfilled in the tank

m_r : Effective mass of fluid for rocking motion

m_{rf} : Mass of tank roof

m_{sh} : Mass of tank shell

R_b : Length between origin *O* and gravity center of m_b

R_{bpUL} : Length between origin *O* and gravity center of m_{bpUL}

R_{bpNUL} : Length between origin *O* and gravity center of m_{bpNUL}

R_{rb} : Length between origin *O* and gravity center of m_{rb}

R_{rf} : Length between origin *O* and gravity center of m_{rf}

R_{sh} : Length between origin *O* and gravity center of

m_{sh}

R_r : Length between origin O and gravity center of m_r

$S_{AH}^{ratio}(T_b, h)$: a ratio of response acceleration to the ground acceleration

T_b : Natural period of the tank bulging motion

$(\ddot{z}_H)_{\max}$: Maximum horizontal ground acceleration

α_b : Angle between vertical line y and R_b

α_{rb} : Angle between vertical line y and R_{rb}

α_{bpUL} : Angle between vertical line y and R_{bpUL}

α_{bpNUL} : Angle between vertical line y and R_{bpNUL}

α_{rf} : Angle between vertical line y and R_{rf}

α_{sh} : Angle between vertical line y and R_{sh}

α_r : Angle between vertical line y and R_r

9. References

[1] Malhotra, P. K., and Veletsos, A. S., 1994, "Uplifting response of unanchored liquid-storage tanks," J. Struct. Div. ASCE, 120(12), pp. 3525–3547.

[2] Clough, D. P., 1977, "Experimental evaluation of seismic design methods for broad cylindrical tanks," UCB/EERC-77/10, PB-272 280.

[3] Eurocode 8, 2006, Design of structures for earthquake resistance, Part 4: Silos, tanks and pipelines, BS EN 1998-4:2006, p. 73.

[4] Taniguchi, T., 2004, "Experimental and analytical studies of rocking mechanics of unanchored flat-bottom cylindrical shell model tanks," Proc. Seismic Engineering, ASME, 486-1, pp. 119-127.

[5] Taniguchi, T., Okui, D., 2014, "A case study of evaluation of tank rock motion with simplified analysis procedure," Proc. Seismic Engineering, ASME, Paper No. PVP2014-28635.

[6] Taniguchi T, Katayama Y., 2016, "Masses of fluid for cylindrical tanks in rock with partial uplift of bottom plate," ASME. J. Pressure Vessel Technol. 138(5):051301-051301-13. doi:10.1115/1.4032784.

[7] Nakashima, T., 2012, "Study on uplift of flat-bottom cylindrical shell tank based on static large deformation implemented by semi-analytical finite element analysis," Ph. D. dissertation at Tottori University. (Japanese)

[8] Taniguchi, T., 2005, "Rocking mechanics of flat-bottom cylindrical shell model tanks subjected to harmonic excitation," J. Pressure Vessel Technol., ASME, 127(4), pp. 373-386.

[9] Taniguchi, T., Nakashima, T., Yoshida, Y., 2016, "Contribution of the bending stiffness of the tank bottom plate and out-of-round deformation of cylindrical shell to the tank rocking motion," Proc. Seismic Engineering, ASME, PVP2016-63916.

[10] Taniguchi T., 2004, "Experimental and analytical study of free lift-off motion induced slip behavior of rectangular rigid bodies," ASME. J. Pressure Vessel Technol. 126(1):53-58. doi:10.1115/1.1636785.

[11] Taniguchi, T., Mentani, Y., and Komori, H., 2000, "The lift-off response of an unanchored flat-bottom cylindrical shell tank subjected to horizontal excitation and its slip criteria," Seismic Engineering, PVP-Vol. 402-2, ASME, New York, pp. 159–165.

[12] T. Taniguchi, T. Murayama, Y. Mentani, H. Komori, T. Yoshihara, 2000, "Slip verification method for the flat-bottom cylindrical shell tank subjected to horizontal and vertical ground motion," Journal of structural mechanics and earthquake engineering, No. 661/I-53, 95-105, JSCE. (Japanese)

[13] Taniguchi T, Segawa T., 2013, "Fundamental Mechanics of Walking of Unanchored Flat-Bottom Cylindrical Shell Model Tanks Subjected to Horizontal Harmonic Base Excitation," ASME. J. Pressure Vessel Technol. 135(2):021201-021201-7. doi:10.1115/1.4007289.

[14] Vibration Handbook for Civil Engineers, 1985, JSCE, pp. 414-415. (Japanese)

[15] Taniguchi, T., Nakashima, T., Okui, D., 2015, "Approximation of uplift of flat-bottom cylindrical tanks and effects of out-of-plane deformation of cylindrical shell on it," Proc. Seismic Engineering, ASME, Paper No. PVP2015-45083.